

Improved black-winged kite algorithm and finite element analysis for robot parallel gripper design

Advances in Mechanical Engineering
2024, Vol. 16(10) 1–16
© The Author(s) 2024
DOI: 10.1177/16878132241288402
journals.sagepub.com/home/ade



Ma Haohao^{1,2}, Azizan As'arry², Feng Yanwei¹,
Cheng Lulu¹, Aidin Delgoshaei², Mohd Idris Shah Ismail²
and Hafiz Rashidi Ramli³

Abstract

This paper presents a comprehensive study on the design optimization of a robotic gripper, focusing on both the gripper modeling and the optimization of its parallel mechanism structure. This study integrates the Black-winged Kite Algorithm (BKA), Finite Element Analysis (FEA), Backpropagation Neural Network (BPNN), and response surface optimization techniques. The Good Point Set (GPS), nonlinear convergence factor, and adaptive t-distribution method improve BKA, which enhances exploration and exploitation performance, convergence speed, and solution quality. Subsequently, the parallel mechanism structure is designed to minimize the total mass, total deformation, and maximum equivalent stress. The central composite design (CCD) method was used to design the FEA experiment and establish the BKA-BPNN regression prediction model. The RMSE of this model's training set and test set are 0.001615 and 0.0029328. A response surface optimization model is constructed to determine the best design solution. The optimized design achieves a 33.12% reduction in maximum equivalent stress, a 1.47% decrease in total mass, and a 0.16% reduction in maximum total deformation. This study provides valuable insights into the design optimization process for robotic grippers, showcasing the effectiveness of the proposed methodologies in enhancing performance while reducing mass and improving structural integrity.

Keywords

Robot gripper, black-winged kite algorithm, finite element analysis, neural network, central composite design

Date received: 9 May 2024; accepted: 14 September 2024

Handling Editor: Sharmili Pandian

Introduction

In the field of robot research, specific tasks must be achieved through robot end effectors. Among the many end effectors, grippers that mimic human manual dexterity are particularly important for their versatility and adaptability in handling a variety of objects. Grippers can perform tasks such as grasping, manipulating, and transporting objects. A key design aspect of this type of clamp is the mechanism used to securely clamp the object, which directly affects its performance and efficiency.

¹Department of Mechanical Engineering, Faculty of Electromechanical Engineering, Tianshui Normal University, Tianshui, China

²Department of Mechanical and Manufacturing Engineering, Faculty of Engineering, Universiti Putra Malaysia, Serdang, Malaysia

³Department of Electrical and Electronic Engineering, Faculty of Engineering, Universiti Putra Malaysia, Serdang, Malaysia

Corresponding author:

Azizan As'arry, Department of Mechanical and Manufacturing Engineering, Faculty of Engineering, Universiti Putra Malaysia, Serdang, Selangor 43400, Malaysia.

Email: zizan@upm.edu.my



Creative Commons CC BY: This article is distributed under the terms of the Creative Commons Attribution 4.0 License (<https://creativecommons.org/licenses/by/4.0/>) which permits any use, reproduction and distribution of the work

without further permission provided the original work is attributed as specified on the SAGE and Open Access pages (<https://us.sagepub.com/en-us/nam/open-access-at-sage>).

Parallel gripper mechanisms have become an important solution for achieving stable and robust gripping in robotic systems. Using a parallelogram kinematic structure can provide balanced force distribution and precise control of the grasping operation, thereby improving efficiency and reliability for various tasks. The importance of parallel gripper mechanisms lies in their ability to mimic the coordinated movements of human fingers, allowing robots to interact with objects like human manipulation.¹

In recent years, a large amount of research effort has been devoted to optimizing the design and performance of robotic grippers, with a particular focus on addressing challenges related to design methods, optimization algorithms,² and structural analysis techniques.³ Vaisi et al. reviewed the application of robots in industrial production and introduced the future research trends of robots.⁴ Jin and Han introduced the huge potential of robotic arms in agricultural development, which uses different hardware to achieve multiple functions to help agricultural development in the new era.⁵ Jung and Shin studied the help of nursing robots for the aging population, including functions such as assisted mobility, toileting, monitoring, and communication.⁶ Gao et al. developed a robot end effector for tomato picking, which uses pneumatic control, and the success rate of automatic picking reaches 70.1%.⁷ Cvitanic et al. proposed a robot end effector using laser tracker and inertial sensor fusion, which takes into account speed and angular acceleration to improve the working accuracy of the robot end effector significantly.⁸ Chang et al. studied a multi-degree-of-freedom wrist robot end effector, which can avoid motion singularities and achieve better flexibility.⁹ Dörterler et al. proposed a multi-strategy optimization method for designing robot grippers and obtained the optimal design parameters for robot grippers.¹⁰ AboZaid et al. reviewed the materials and grasping technologies of soft material robot grippers and discussed the application of robot grippers.¹¹

Scholars have conducted control and application research on robots and explored a variety of application scenarios and design methods. Design methods include more mathematical modeling of robot grippers, but less combining the optimal design parameters with structural design and verification, making it difficult to better understand its kinematics and dynamics. Black-winged Kite Algorithm (BKA) has been used to solve complex optimization problems such as engineering optimization, path planning, and scheduling problems. In the field of robot design, the application of BKA is still in the initial exploration stage. This study applies BKA to the design and optimization of robot grippers, making full use of its advantages in exploration and development to find the optimized design parameters. This innovative application not only expands the application scope of BKA, but also provides a new

optimization method for robot gripper design. The application of the BKA can optimize the design of the gripper by effectively exploring the design space and determining the best solution. Finite Element Analysis (FEA) has been widely used to evaluate the structural integrity and performance of grippers under different operating conditions, allowing researchers to identify design flaws and improve overall efficiency. In addition, the Back Propagation Neural Network (BPNN) model can efficiently predict the results of interest for multiple design schemes.

This paper aims to contribute to the existing body of knowledge by proposing a new method for designing and optimizing robot grippers with parallel kinematic structures. Specifically, the research focuses on the mathematical modeling of the clamp mechanism, the application of heuristic optimization algorithms to enhance clamp performance, and the use of FEA to verify the structural integrity of the proposed design. The BKA-BPNN model is established to accurately predict the performance of the parallelogram mechanism under different design schemes. The optimal design parameters are determined by response surface optimization, which significantly improves the performance indicators of the gripper. Finally, a physical prototype is manufactured according to the optimal parameters, and multiple experiments are carried out to verify the effectiveness of this design. Potential innovations and contributions of this study include:

- (1) An improved BKA is proposed to optimize the mathematical model of the gripper mechanism. FEA is used to further refine the mass, stress and structural parameters of the design.
- (2) Development of a BKA-BPNN model to accurately predict the performance of the gripper under different design scenarios, demonstrating the effectiveness of the neural network model.
- (3) Response surface optimization was used to determine the optimal design parameters, significantly improving the gripper's clamping force, mass, and maximum equivalent stress performance indicators.
- (4) A comprehensive approach to design and optimize a robotic parallel gripper was proposed by integrating improved BKA, FEA, BPNN, and response surface optimization techniques.

By integrating these aspects, this study aims to provide insights into the design and optimization of parallel grippers for robotic applications, ultimately improving robot manipulation capabilities in various industrial and research fields. The robot gripper designed in this study has an actuation force limited to 50 N and targets specific tasks in electronic manufacturing, precision assembly, and light material handling.

The contents of this paper are: Section 2 introduces the methodology related to this research, including robot gripper modeling, black-winged kite algorithm and its improvements, experimental design methods, neural network, and response surface optimization methods; In section 3, a case design of the robot gripper was carried out, the structure of the parallel gripper was optimized, and the correctness of the design was verified; Section 4 summarizes the significance of this study and the extension of the design methodology.

Research method

This section provides a comprehensive overview of the methodology employed in this study to support the design and optimization of robotic parallel grippers. Figure 1 presents the work route of this research, with methods ranging from theoretical modeling to practical experiments.

Robot gripper modeling

Robotic grippers are designed taking into account the required clamping force, precision and stability to meet the needs of a specific application. The structure needs to be sufficiently rigid and stable while remaining flexible enough to accommodate objects of different shapes and sizes. Taking into account the special environment in which the robot operates, stainless steel materials are selected to increase the service life of the gripper.

Two primary approaches commonly employed for gripper actuation include direct motor-to-gear transmission and motor-to-screw mechanism driving a sliding block. While both methods offer their unique advantages, the latter, involving motor-driven screw mechanisms, has garnered significant attention in robotic gripper design. As shown in Figure 2, by leveraging the self-locking properties of screw mechanisms, robotic grippers can achieve enhanced stability and holding force, thus facilitating the manipulation of objects with varying shapes and sizes in diverse operational environments.¹⁰

Fk denotes the gripping force of the robot gripper when working. $a, b, c,$ and δ denote the link structural parameters of the robot gripper. $e, f,$ and l denote the position structural parameters of the robot gripper. These parameters are all variables for the optimal design of the robot gripper. $z, \alpha,$ and β denote a certain moment of the motion state. At any moment, record the length of point A to point C as g , and the angle $\angle CAD$ as φ . The parameters of the structure can be calculated, expressed as equations (1)–(4).

$$g = \sqrt{(l - z)^2 + e^2} \quad (1)$$

$$\alpha = \arccos\left(\frac{a^2 + g^2 - b^2}{2ag}\right) + \varphi \quad (2)$$

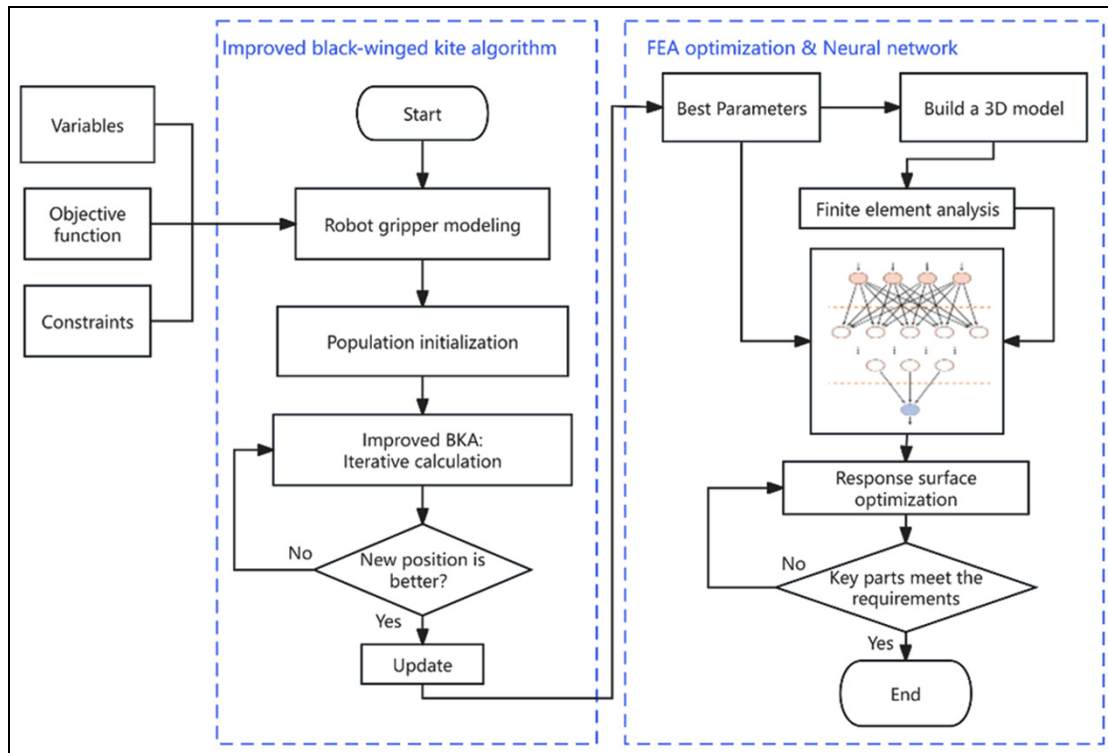


Figure 1. Flow chart for robot gripper optimization.

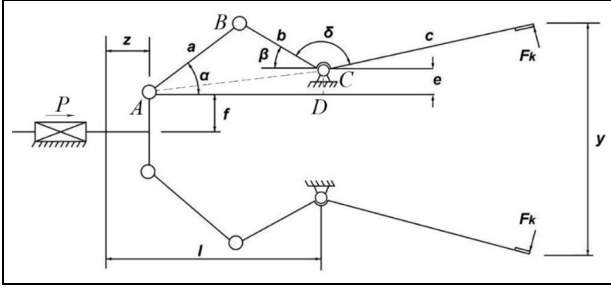


Figure 2. Motion diagram of robot gripper.

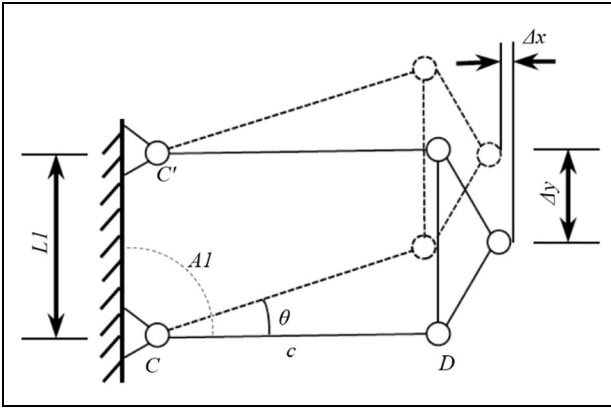


Figure 3. The parallelogram mechanism of the gripper.

$$\beta = \arccos\left(\frac{b^2 + g^2 - a^2}{2bg}\right) - \varphi \quad (3)$$

$$\varphi = \arctan\left(\frac{e}{l-z}\right) \quad (4)$$

When the driving force of the motor screw is P , calculate the static balance between the force passing through the connecting link a and the gripping force Fk , and then Fk can be calculated, as equation (5).

$$Fk = \frac{Pbsin(\alpha + \beta)}{2c \cos(\alpha)} \quad (5)$$

Consider the displacement y of the gripper, which is related to the opening and closing angle of the link c and the position parameters e, f . y can be calculated as equation (6).

$$y = 2(e + f + c \sin(\beta + \varphi)) \quad (6)$$

To realize the parallel gripping capability of the robot gripper, a parallelogram mechanism needs to be designed, as shown in Figure 3. Add a fixed point C' , the distance between point C and point C' is Ll , and the horizontal angle of CC' is Al . Δy is the opening and closing distance of the holding, and Δx is the Level difference during opening and closing.

Improved black-winged kite algorithm

The Black-winged Kite Algorithm (BKA) is a heuristic optimization algorithm proposed by Wang et al. in 2024.¹² It was inspired by the migration and hunting behavior of the black-winged kite. BKA has proven its ability to achieve the best performance in 66.7, and 72.4 of the CEC-2022 and CEC-2017 test functions with its excellent performance. After the BKA was proposed, some researchers began to use this algorithm to solve various optimization problems, including engineering design and machine learning.

Like most other heuristic optimization algorithms, the population is initialized by randomly assigning the position of each black-winged kite. The black-winged kite adjusts the angle of its wings and tail according to the wind speed during flight, hovers quietly to observe its prey, and then quickly dives to attack. The strategy includes different attack behaviors for global exploration and search. The migratory behavior of the black-winged kite is through a dynamic selection of superior leaders. If the fitness value of the current population is greater than the fitness value of the random population, the population will be guided to the destination to ensure the success of the migration.

In this study, based on the robot gripper problem, the original BKA was improved and upgraded to alleviate the shortcomings of BKA in the problem of premature convergence, easy falling into local optimality, and low convergence accuracy.

The improved BKA (I-BKA) uses the Good Point Set (GPS) method for population initialization.¹³ For problems with i populations and j dimensions, the method of finding the optimal point set is shown in the equation (7).

$$\begin{cases} r_j^i = \text{mod}\left(2 \cos\left(\frac{2\pi j}{k}\right), i, 1\right) \\ k = 2j + 3 \\ P_j^i = lb_j + r_j^i(ub_j - lb_j) \end{cases} \quad (7)$$

P_j^i is the good point set of the i population in the j dimension, where lb_j and ub_j are the lower and upper bounds of the j -th variable. Figure 4 compares the initialization results of 100 populations in 2-dimensional space using the GPS method and randomly generated populations. It can be seen that the population initialization distribution of the GPS method is more uniform.

During the attack behavior stage of the black-winged kite, the original BKA selected the constant $p = 0.9$ as the judgment condition to update the population position. This study adaptively selected probability p according to the nonlinear convergence factor to adjust the position update, which is calculated as shown in equation (8). The nonlinear convergence factor can better control the step size or perturbation

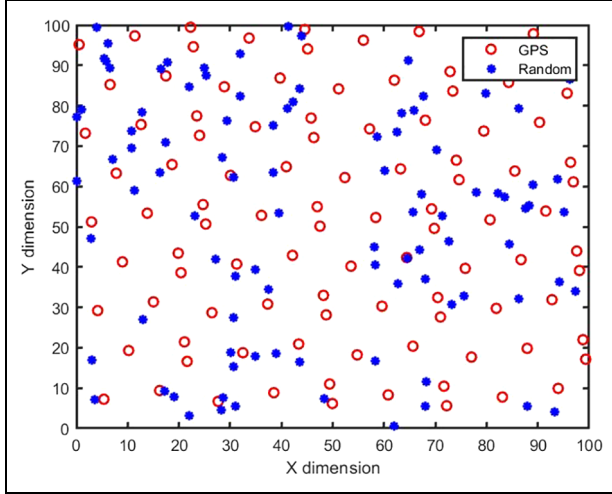


Figure 4. Comparison of population initialization.

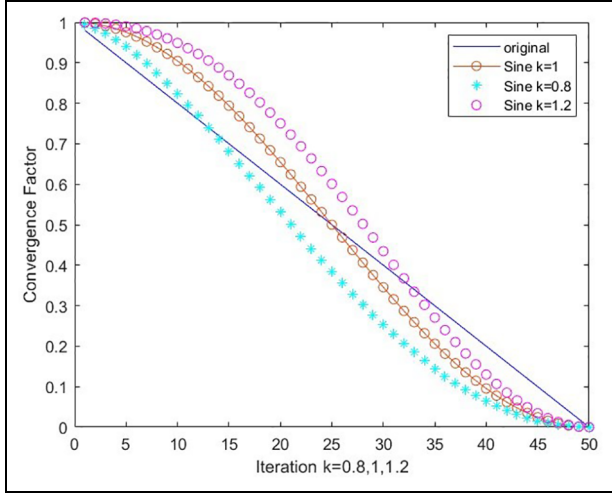


Figure 5. Non-linear convergence factor.

size of the algorithm during the search process, thereby achieving a balanced relationship between exploration and exploitation.

$$p = \frac{1}{2} + \frac{\sin(\frac{\pi}{2} + \pi(\frac{t}{T})^k)}{2} \quad (8)$$

where T is the maximum number of iterations, t is the current number of iterations. Figure 5 depicts the convergence factor of the sinusoidal nonlinearity for different values of parameter k . The convergence factor is used to adjust the step size in the optimization algorithm. In this study, $k = 0.8$, which allows the algorithm to conduct a large-scale exploration in the early stage and focus on the development near the excellent solution in the later stage, thereby increasing the probability of finding the global optimal solution.

The original BKA uses Cauchy distribution to dynamically select excellent leaders in migration behavior to ensure the success of migration. This process solves the risk of falling into the local optimal solution during the BKA algorithm solution process. Based on the original BKA, the t distribution variation is used to help the algorithm increase randomness in the migration stage and help jump out of the local optimal solution. The formula is shown in (9).

$$X_{i,j}^{t+1} = X_{i,j}^t + X_{i,j}^t \text{trnd} \left(e^{\left(\frac{t}{T}\right)^2} \right) \quad (9)$$

Here X_{ij}^t denotes the position obtained by the i -th black-winged kite in the t -th iteration of the j -th dimensional space. trnd denotes the Student's t random numbers. Based on the population initialization and nonlinear convergence factor of the Good Point Set (GPS) method, a variety of mutation strategies were tried, including Gaussian mutation, Cauchy mutation, adaptive t distribution, normal cloud distribution, and non-uniform mutation. After running the CEC2017 function many times, it was found that the adaptive t distribution had the best improvement effect. Figure 6 plots the convergence curves to compare the performance differences of each strategy, where Figure 6(a) is the CEC2017 F23 function, and Figure 6(b) shows the convergence curves of 10 average runs under different mutation strategies. The Gaussian mutation, Cauchy mutation, adaptive t distribution, normal cloud distribution, and non-uniform mutation strategies in the legend are Gauss-BKA, Cauchy-BKA, Self-t-BKA, Cloud-BKA, and H-BKA, respectively.

Adaptive t -distribution mutation dynamically adjusts the degree of freedom parameter of t -distribution, so that the mutation strategy can adaptively adapt to different stages of the search process. In the early stage, the t -distribution with lower degrees of freedom can introduce larger random perturbations and enhance the global search capability; in the later stage, the degrees of freedom gradually increase, making the mutation more refined and helpful for local development. Multiple running results show that adaptive t -distribution mutation is superior to other mutation strategies in terms of convergence speed and solution quality.

Neural network regression analysis

Neural networks are composed of interconnected nodes organized into layers and are good at capturing complex patterns and relationships in data.¹⁴⁻¹⁶ Through training, a neural network iteratively adjusts its internal parameters to minimize prediction errors and improve performance on a specific task.^{17,18}

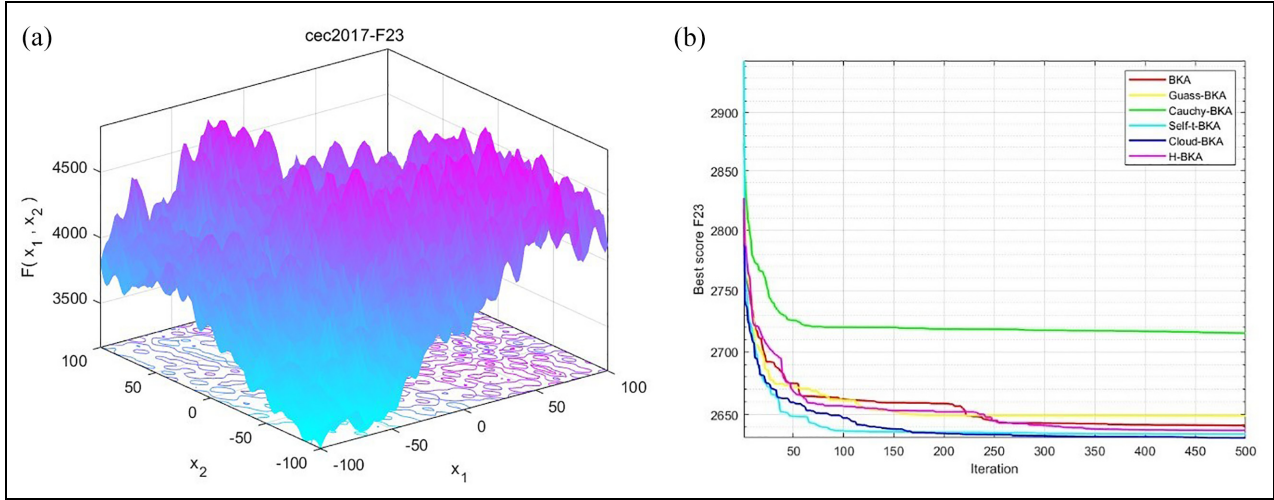


Figure 6. Convergence curves of different mutation strategies: (a) F23 function and (b) convergence curves of F23 function.

This study chose a neural network regression analysis, specifically the backpropagation neural network (BPNN), to model the parallelogram mechanism in robot fixture design. The structure of BPNN is shown in Figure 7.

The calculation of BPNN output \hat{y}_i is as equation (10), where b_{ij} and w_{ij} represent the bias and weight of the neuron.

$$\hat{y}_i = f\left(\sum_{i=1}^n w_{ij}x_i - b_{ij}\right) \quad (10)$$

Calculate the total error E of the total output value according to equation (11), that is, the calculated output value \hat{y}_j and the true value y of the data set.

$$E = \sum_{i=1}^n (\hat{y}_i - y_i)^2 \quad (11)$$

Gradient descent techniques can then be used to minimize weights, as in equation (12), where η is the learning rate.

$$w_{ij} = w_{ij} - \eta \frac{\partial E(w_{ij})}{\partial w_{ij}} \quad (12)$$

BPNN can provide a flexible and versatile regression analysis method. When designing the parallelogram structure of the robot gripper, the influence of the linker length, linker angle, and linker material thickness parameters on the working intensity will be considered. Each design option has an impact on the total mass and deformation of the structure. Using BPNN to perform regression analysis on each solution, the prediction results are very meaningful and can help select a more appropriate design solution.

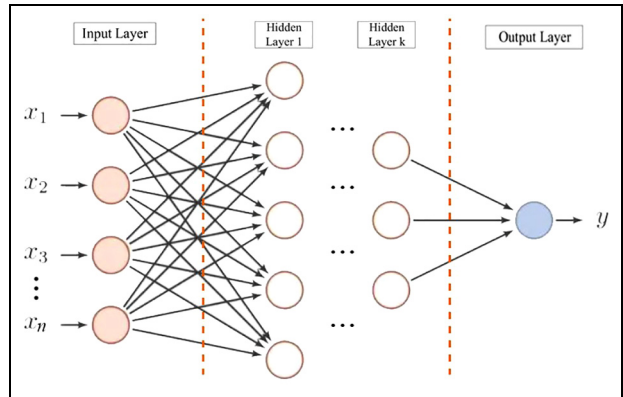


Figure 7. Backpropagation neural networks (BPNN) structure.

In this study, the choice of BPNN has its unique advantages over other types of neural networks. BPNN has a simple structure and is trained using the gradient descent algorithm, which can efficiently minimize the prediction error. Compared with some complex deep neural networks, the training process of BPNN is relatively simple and fast, ensuring that the performance of the manipulator can be effectively predicted accurately.

However, BPNN may suffer from slow convergence and overfitting problems, and this study proposes an improved method that combines BPNN with improved BKA. Figure 8 shows the improved BKA-BPNN process. By taking advantage of BKA's efficient and adaptive search capabilities, the proposed method improves the convergence speed, enhances the exploration-exploitation trade-off, and improves the robustness to noisy data, making it a good solution to the problem of robot gripper design. regression problem.

Optimizing the initialization weights of BPNN using BKA provides a more effective and efficient method of

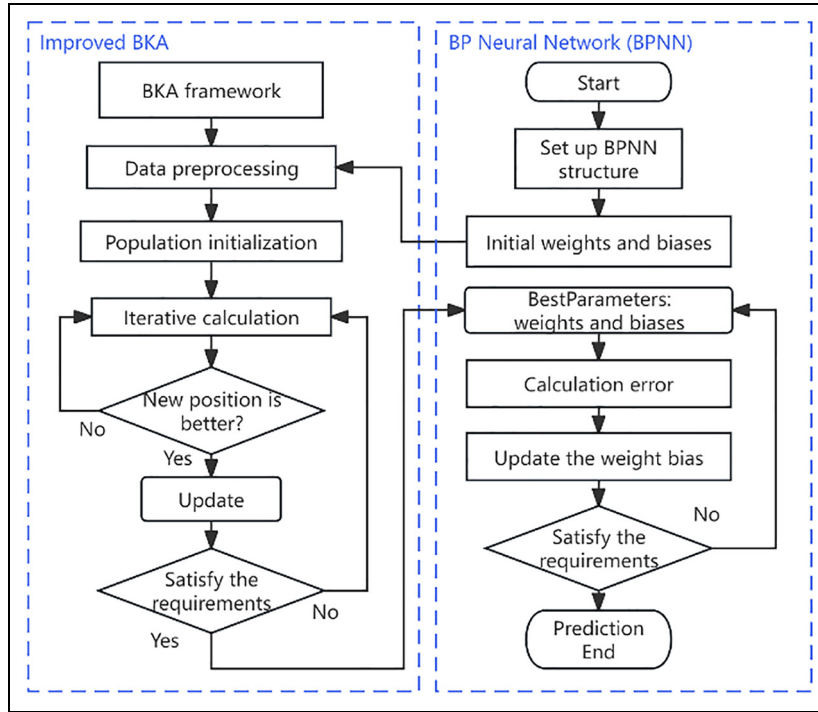


Figure 8. Flow chart of improved BKA-BPNN.

initializing neural network parameters. Traditional methods of initializing weights (such as random or uniform distributions) can result in suboptimal solutions and slow convergence during training. By leveraging BKA's adaptive search strategy, initialization weights can be optimized to better align with the problem space, thus promoting faster convergence and improving solution quality.

Response surface optimization

In the design of the robot gripper, to better determine the parallelogram mechanism parameters and profile size parameters, the response surface optimization method is used to find the optimal solution. This method collects and analyzes a series of experimental data and establishes a response surface model to construct a mathematical model to approximate the relationship between design parameters and performance indicators.¹⁹

Response surface models usually use the Central Composite Design (CCD)²⁰ and Box-Behnken Design (BBD),²¹ then use polynomial functions, radial basis functions, or neural networks to fit experimental data. In this study, CCD was used to construct a response surface model, and second-order polynomials were used for fitting. CCD combines full factorial design with additional center points and pivot points to ensure a wider design space with fewer experiments. Second-order polynomials as the fitting function of the response

surface model can effectively capture the nonlinear relationships in experimental data and avoid the overfitting problem that may be introduced by higher-order polynomials. The second-order polynomial constructs the response surface model, and the equation is shown in equation (13).

$$Y = \beta_0 + \sum_{i=1}^n \beta_i X_i + \sum_{i=1}^n \beta_{ii} X_i^2 + \sum_{i=1, i \leq j}^n \beta_{ij} X_i X_j + \varepsilon \quad (13)$$

Among them, Y is the response variable, X_i is the independent variable, β_0 is the constant term, β_i is the linear term coefficient, β_{ii} is the quadratic term coefficient of the independent variable X_i , β_{ij} is the cross-term coefficient of the independent variables X_i and X_j , and ε is the error term. Constructing a response surface can intuitively present the relationship between the response variables and independent variables in the form of images. The response surface model optimization constructed by CCD and second-order polynomials can provide reliable choices for the design of mechanical grippers.

Results and discussion

In this section, a certain model of a robot gripper is selected as the design object, and various heuristic algorithms are compared to solve the problem. The optimal

solution is selected through a comprehensive discussion of the designed parameters, and the parallel gripping function of the gripper is realized.

Optimization calculation

According to the established robot gripper model optimization problem constraints, the key parameters are solved with the minimum change in gripping force as the goal. These key parameters include structural variables such as connecting rod length and position. In addition, performance indicators including clamping force, stability, and efficiency were established to evaluate the effectiveness of the parameters.

For the robot gripper model selected in this study, given the motor driving force $p = 50$ N, other parameters of the robot gripper are designed. The design variables are in equation (14), the objective function is in equation (15), and the constraints are in equation (16).

$$\mathbf{X} = (x_1, x_2, x_3, x_4, x_5, x_6, x_7) = (a, b, c, e, f, l, \delta) \quad (14)$$

$$\text{Minimize } f(\mathbf{X}) = -\min_z F_k(\mathbf{X}, Z) + \max_z F_k(\mathbf{X}, Z) \quad (15)$$

$$\text{Subject to } \begin{cases} g_1(\mathbf{X}) = -Y_{min} + y(\mathbf{X}, Z_{min}) \leq 0 \\ g_2(\mathbf{X}) = -y(\mathbf{X}, Z_{max}) \leq 0 \\ g_3(\mathbf{X}) = Y_{max} - y(\mathbf{X}, 0) \leq 0 \\ g_4(\mathbf{X}) = y(\mathbf{X}, 0) - Y_G \leq 0 \\ g_5(\mathbf{X}) = l^2 + e^2 - (a + b)^2 \leq 0 \\ g_6(\mathbf{X}) = b^2 - (a - e)^2 - (l - Z_{max})^2 \leq 0 \\ g_7(\mathbf{X}) = Z_{max} - l \leq 0 \end{cases} \quad (16)$$

The values here are $Y_{min} = 50$, $Y_{max} = 100$, $Y_G = 150$, $Z_{max} = 100$. The bounds of the design variables are: $20 \leq a \leq 100$, $30 \leq b \leq 100$, $100 \leq c \leq 200$, $10 \leq e \leq 100$, $10 \leq f \leq 30$, and $50 \leq l \leq 200$, $\pi/2 \leq \delta \leq \pi$.

To ensure the accuracy of the optimization calculation and the effectiveness of the improved BKA algorithm, a variety of heuristic optimization algorithms were implemented to solve this robot gripper model optimization problem. Other heuristic algorithms include the Dung Beetle Optimizer (DBO) algorithm,²² the Harris Hawks Optimization (HHO) algorithm,²³ and the Gray Wolf Optimization (GWO) algorithm.²⁴ Each algorithm is iterated to search for the best solution in the same design space. The comparative convergence curve is shown in Figure 9. In the calculations, the population number was set to 30, and the maximum number of iterations was set to 500.

The improved BKA shows excellent performance in solving the robot gripper optimization problem, surpassing other algorithms in terms of convergence.

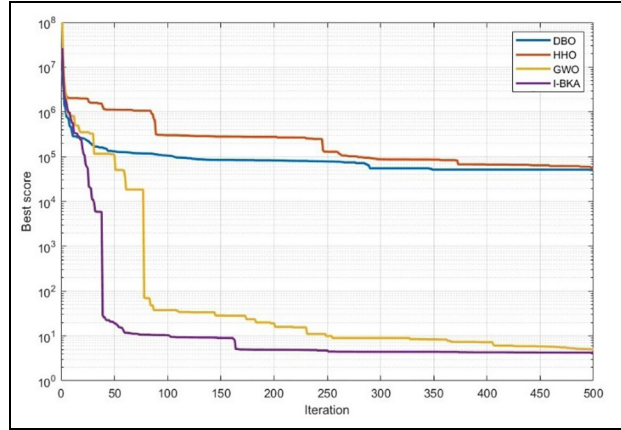


Figure 9. Convergence curves for robotic gripper design.

BKA convergence curves show faster convergence speeds and smoother convergence trajectories compared to other optimization techniques. This superior performance can be attributed to BKA's ability to effectively explore the solution space while effectively exploiting promising regions, resulting in faster and more consistent convergence to the optimal solution.

The optimal solutions and mean comparison values solved by different algorithms are shown in Table 1, which respectively shows the worst value, optimal value, standard deviation value, average value, and median value of different algorithms. Table 2 presents the variable optimal solutions obtained by the four algorithms.

The convergence results demonstrate the effectiveness of the improved BKA in solving the design optimization of robotic grippers. To facilitate the continued design of the robot gripper, the obtained design variables are summarized as $\mathbf{X} = (a, b, c, e, f, l, \delta) = (100, 85, 120, 10, 25, 100, 105)$.

Parallelogram gripping mechanism

After finalizing the overall dimensions of the gripper, attention turned to the design of the actuation mechanism to achieve parallel gripping, known as the parallelogram mechanism. Drawing inspiration from existing parameters of parallelogram mechanisms, simulations were conducted to analyze the load-bearing characteristics under operational conditions.

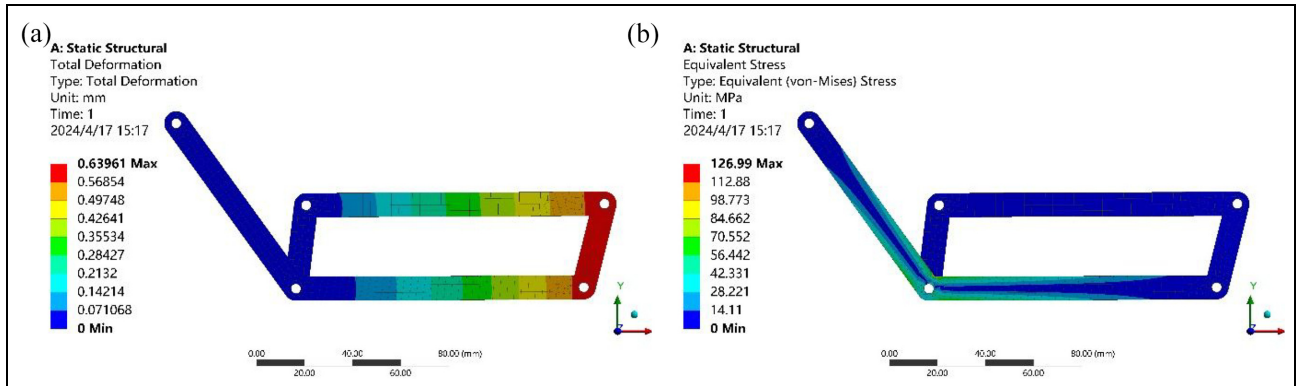
Referring to the gripper in Figure 3, when it grips the object, it generates force and moment on point D . In this study, it is assumed that the supporting force is 50 N and the offset distance of the force is 50 mm, then the moment applied on point D is 250 N·mm. Apply this load condition to the parallelogram mechanism and obtain its FEA results, as shown in Figure 10. Figure 10(a) shows the total deformation under the

Table 1. Optimal solution and mean comparison of algorithm solution.

Name	I-BKA	DBO	HHO	GWO
Worst	4.010218788	4.244410828	1018.872605	4.286281804
Best	4.440081641	253658.3464	187966.1084	6.959525306
Std	0.17514738	113436.8138	76521.43803	1.101789248
Mean	4.261542521	50736.40494	55464.74408	5.012970231
Median	4.268047556	4.463612474	33112.29566	4.562299487

Table 2. Optimize the results of calculated variables.

Method	a (mm)	b (mm)	c (mm)	e (mm)	f (mm)	l (mm)	δ (deg)
I-BKA	99.32303122	88.82640175	106.7638743	10	27.28784101	100.7928933	104.8566526
DBO	100	89.55925621	102.2660319	10	14.85240926	100.6692296	98.270505
HHO	100	46.01051204	140.6353874	15.22102993	12.48763443	98.99681877	93.56850347
GWO	100	88.6404011	109.1843607	10.18606774	28.68392612	111.6884013	107.943737

**Figure 10.** FEA results of the initially designed parallelogram structure: (a) total deformation and (b) equivalent stress.

action of gripping torque, and Figure 10(b) shows the equivalent stress under the gripping working state.

It can be seen that the most dangerous component of the parallel gripping mechanism of the robot gripper corresponds to the connecting link b - δ - c in Figure 2. The width parameter of the connecting rod is set to $R2$. $R2$ and the parameters $A1$ and $L1$ in Figure 3 are response surface optimization parameters. The optimization goal is to minimize the total mass and the maximum equivalent stress of the parallelogram mechanism.

The CCD method is used for experimental design, and the influence of three factors ($L1$, $A1$, $R2$) on the maximum total deformation, maximum equivalent stress, and total mass is analyzed. Variable value range: $31.5 \leq L1 \leq 38.5$, $74.7 \leq A1 \leq 91.3$, $4.5 \leq R2 \leq 5.5$. The 15 sets of experimental results are shown in Table 3.

After obtaining experimental data related to the length ($L1$), angle ($A1$), material width ($R2$), overall structural mass, maximum deformation, and maximum

equivalent stress, BKA-BPNN regression is used to predict a variety of different design options.

BKA-BPNN regression prediction

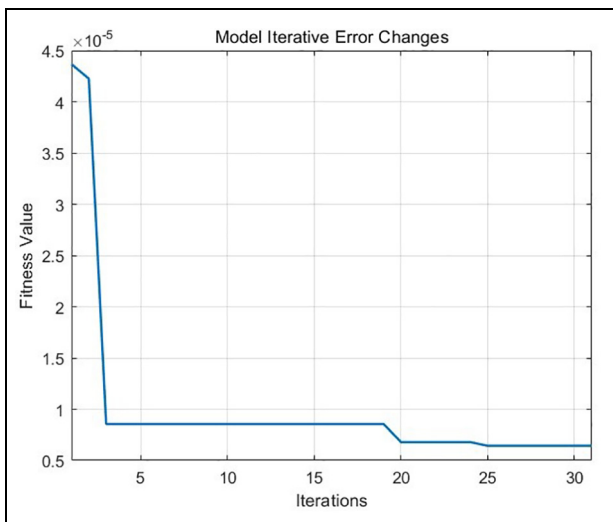
In the design of robotic grippers, a three-input, two-output framework is adopted, where the length ($L1$), angle ($A1$), and material width ($R2$) serve as inputs, while the overall structural mass and maximum deformation represent the outputs.

The BKA-BPNN framework establishes predictive models for estimating the gripper's performance metrics based on input parameters. By training the BKA-BPNN regression model on historical data encompassing various gripper configurations and corresponding performance measurements, the overall structural mass and maximum deformation of prospective gripper designs can be accurately predicted.

BKA-BPNN is used to train the data of the parallelogram mechanism of the robot gripper. Initialize the parameters of BKA, the evolution generation is 30

Table 3. Experimental results designed by CCD method.

Name	$L1$ (mm)	$A1$ (deg)	$R2$ (mm)	Total deformation (mm)	Equivalent Stress (Mpa)	Geometry Mass (kg)
1	35	83	5	0.63961144	126.9934661	0.162833181
2	31.5	83	5	0.639886797	126.9326451	0.160131904
3	38.5	83	5	0.63967512	127.0380305	0.16553645
4	35	74.7	5	0.639282496	125.1829357	0.163067919
5	35	91.3	5	0.640230177	127.9215767	0.162590071
6	35	83	4.5	0.86969331	114.24314	0.154318257
7	35	83	5.5	0.484871737	110.1924803	0.171408229
8	32.15438117	76.25181821	4.593483025	0.818759876	109.6185329	0.153900351
9	37.84561883	76.25181821	4.593483025	0.819373131	145.1197717	0.15829562
10	32.15438117	89.74818179	4.593483025	0.818960808	118.9152727	0.153512456
11	37.84561883	89.74818179	4.593483025	0.819376438	118.9871953	0.157905844
12	32.15438117	76.25181821	5.406516975	0.508922851	85.11177172	0.167795079
13	37.84561883	76.25181821	5.406516975	0.509089355	94.18700571	0.172190348
14	32.15438117	89.74818179	5.406516975	0.510204055	114.8762382	0.167407183
15	37.84561883	89.74818179	5.406516975	0.509867146	114.9531015	0.171800571

**Figure 11.** Diagram of the fitness curve of BPNN.

generations, and the population size is 5. Through continuous optimization training, the BPNN prediction fitness curve is obtained, as shown in Figure 11.

Through continuous training of the training set data and prediction calculation of the test set data, the Root Mean Square Error (RMSE) comparison of the parallelogram structure prediction of the robot gripper after BKA-BPNN optimization is obtained, as shown in Figure 12. Figure 12(a) shows the RMSE of the training set is 0.001615, indicating that the accuracy of predicting the structural quality and maximum deformation based on the input parameters is very high. Figure 12(b) shows that the RMSE of the test set is 0.0029328, which further confirms the generalization ability of the developed model.

The BKA-BPNN model accurately predicts the performance of the parallelogram mechanism of the robot gripper, which is the basis for response surface design.

By fitting the BKA-BPNN prediction model to the response surface model, it can more intuitively and effectively identify the optimal design configuration to minimize structural mass and maximize stiffness.

Selection of optimal design parameters

A response surface model can be constructed based on the BKA-BPNN predictive model. The model is designed to capture the complex nonlinear relationships between input parameters ($L1$, $A1$, $R2$) and output responses (structural mass, maximum deformation, maximum equivalent stress). As shown in Figure 13(a) is the response surface diagram of $A1$ and $R2$ to the total deformation, Figure 13(b) is the response surface diagram of $L1$ and $R2$ to the total mass of the structure, Figure 13(c) is the response surface diagram of $L1$ and $R2$ to the maximum equivalent stress. Figure 13(d) is the response surface diagram of $A1$ and $R2$ to the maximum equivalent stress.

Through regression analysis and curve fitting technology, a robot parallel gripper response surface model was developed to present the influence behavior of design parameters on the design objectives. Utilizing the developed response surface model, an optimization algorithm is employed to systematically explore the design space and identify numerous samples that yield the desired performance target. The design objectives in this study are to minimize structural mass and minimize equivalent stress.

Figure 14(a) is a sample scatter plot of $L1$ and $A1$ to the total mass of the structure. Figure 14(b) is a sample scatter plot of $L1$ and $R2$ to the total mass of the structure. Figure 14(c) is a sample scatter plot of $L1$ and $A1$ to the maximum equivalent stress of the structure. Figure 14(d) is the sample scatter plot of $L1$ and $R2$ to the maximum equivalent stress.

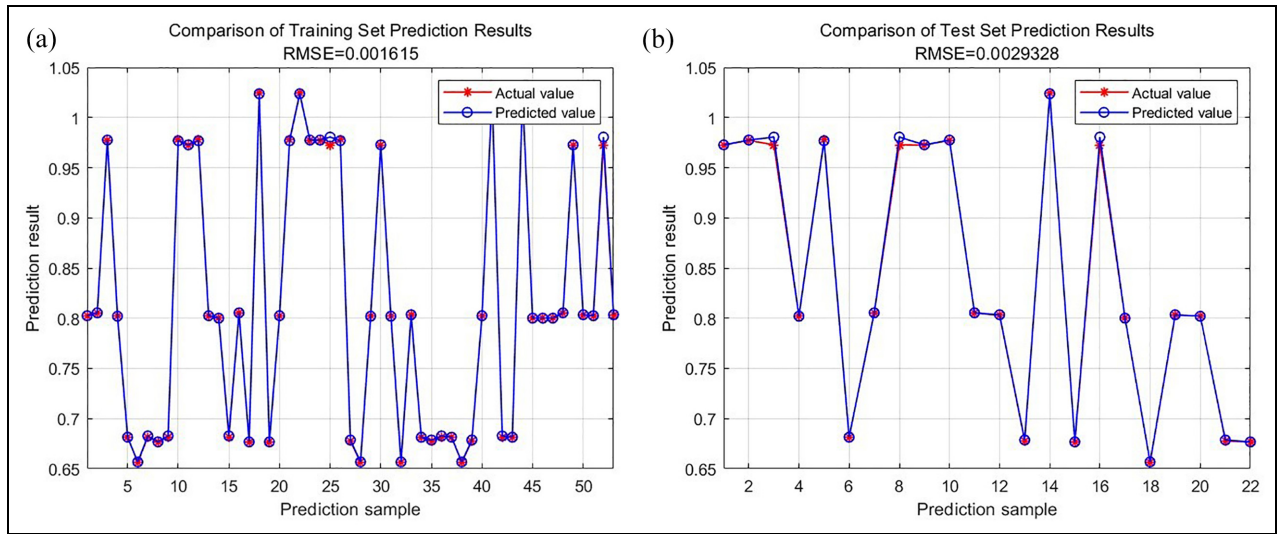


Figure 12. Comparison of prediction result errors: (a) training set prediction results and (b) test set prediction results.

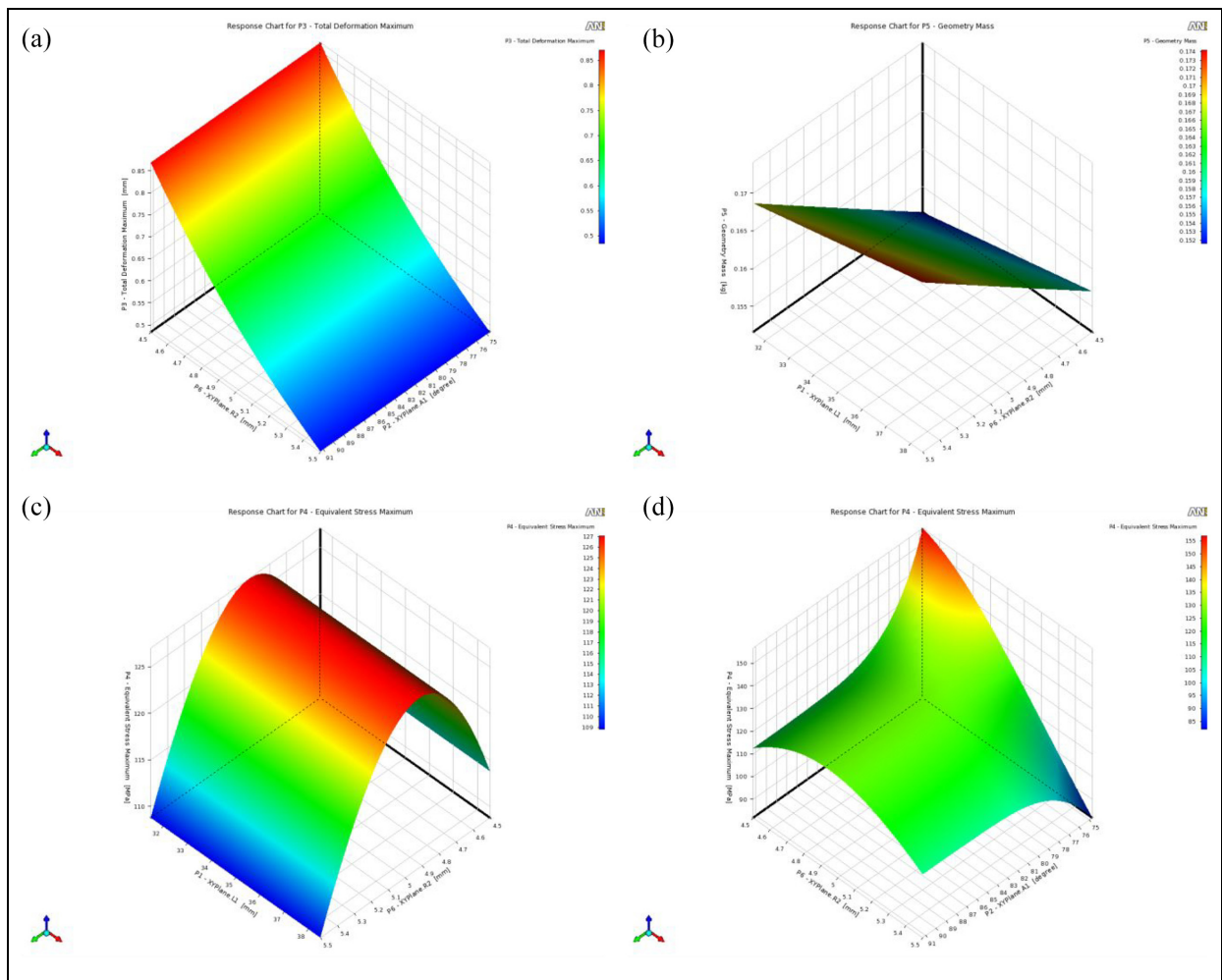


Figure 13. Diagram of response surface model: (a) A1 and R2 to the total deformation, (b) L1 and R2 to the total mass, and (c) L1 and R2 to the equivalent stress, (d) A1 and R2 to the equivalent stress

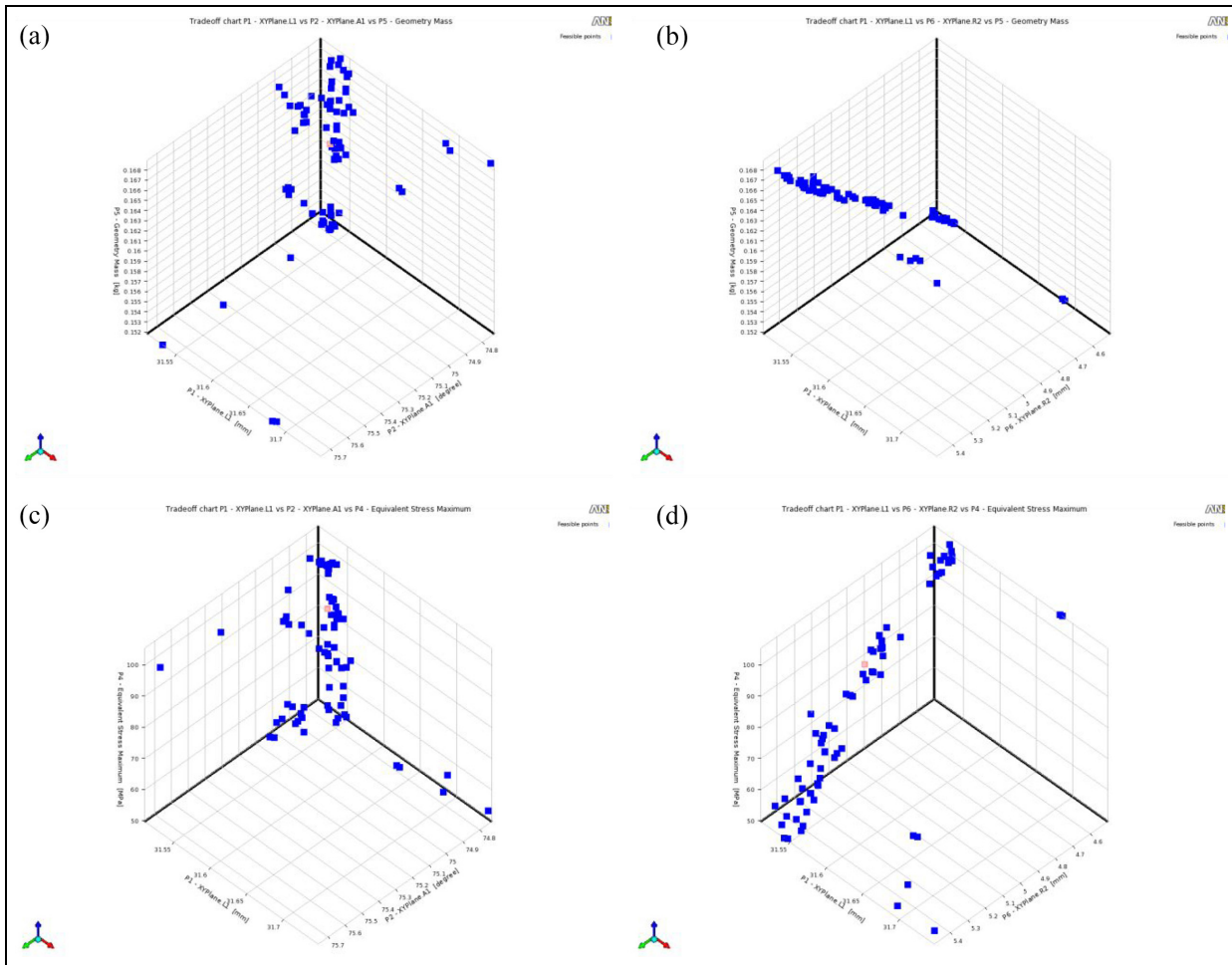


Figure 14. Scatter plot of samples: (a) $L1$ and $A1$ to the total mass, (b) $L1$ and $R2$ to the total mass, (c) $L1$ and $A1$ to the equivalent stress, and (d) $L1$ and $R2$ to the equivalent stress.

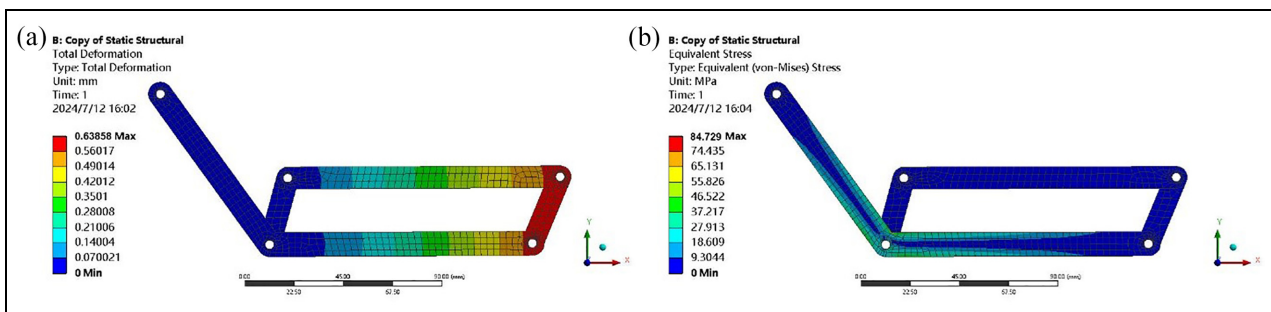


Figure 15. FEA results of the optimized parallelogram structure: (a) total deformation and (b) equivalent stress.

The robot gripper is designed according to the optimal design scheme marked in red in the sample scatter plot, and the FEA results are shown in Figure 15. The values of this design plan are $L1 = 31.535$ mm, $A1 = 74.783^\circ$, $R2 = 5.0026$ mm. Figure 15(a) shows that the total deformation obtained is 0.6385884 mm, Figure 15(b) shows that the maximum equivalent stress

is 84.927 MPa, and the total mass is 0.16043 kg. Compared with the initial plan (total mass 0.16283 kg, maximum total deformation 0.63961 mm, maximum equivalent stress 126.99 MPa, the maximum equivalent stress of the optimized plan is reduced by 33.12%, the total mass is reduced by 1.47%, and the maximum total deformation is reduced by 0.16%.

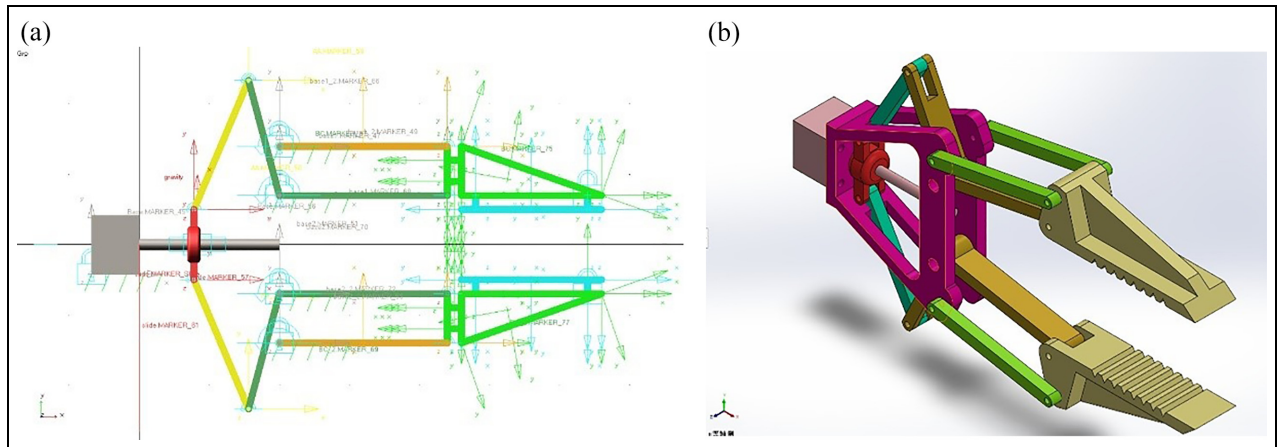


Figure 16. Virtual prototype of the robotic gripper: (a) kinematic design of robot gripper and (b) 3D model of robot gripper.

It can be seen that the use of FEA to evaluate the structural integrity and performance of the robot's parallel gripping mechanism provides valuable data for building a response surface model. Through iterative refinement guided by FEA results, the optimal parameters of the parallelogram mechanism were determined. This comprehensive approach ensures that the parallelogram mechanism not only meets the functional requirements of parallel gripping but also exhibits robustness and reliability under different operating conditions.

Experimental validation

The evaluation of robotic grippers requires multifaceted validation, including gripping force, gripping stability, structural strength, gripping accuracy, and gripping efficiency. This study focused on optimizing stable gripping force as a primary objective. Using an improved BKA, approximate structural parameters were derived, which were further refined through FEA, BKA-BPNN modeling, and response surface analysis. Considerations encompassed part strength, deformation, and overall mass. The operational stability and gripping accuracy of the robotic gripper heavily depend on machining processes, which were not within the scope of this study. Identify optimal solutions through response surface design and transform theoretical designs into a virtual prototype as depicted in Figure 16. Figure 16(a) shows the kinematic pair design of the robot gripper. The structure has nine movable components, 13 low-motion pairs, the degree of freedom is equal to 1, and a motor drives the screw pair of the screw to drive stable movement. Figure 16(b) is the three-dimensional model constructed using computer-aided design (CAD) software, which adopts the dimensions and specifications of the optimal gripper design.

A physical prototype was fabricated to validate the design's functionality after determining the robotic gripper's overall transmission and parallelogram structure dimensions. The drive motor uses a 34 mm stepper motor 42HS34, a T8.2 mm trapezoidal screw with a length of 100 mm and a brass nut. The physical prototype produced is shown in Figure 17, where Figure 17(a) shows the arbitrary state of the gripper, and Figure 17(b) shows the working state of gripping an object.

The experimental setup involved testing the gripping and clamping functionality of the prototype, evaluating its operational stability, and measuring displacement parameters during movement as shown in Figure 18. Figure 18(a) presents the displacement curve of the drive slider and the parallelogram structure during the gripping task, which can be seen that the gripper gradually clamps when the slider moves to the elongation at an average speed. Figure 18(b) shows the displacement curve of the separation of the driving slider and the parallelogram structure after completing the grasping task, which can be seen that when the slide moves to the shortened position at an average speed, the clamps gradually separate. The physical prototype demonstrated reliable operation during gripping and clamping tasks, with smooth and stable motion observed throughout the operational cycle. Displacement parameters were measured to assess the accuracy and consistency of the gripper's movements. The experimental validation confirmed the correctness and effectiveness of the designed robotic gripper, validating its suitability for real-world applications in various industrial and research settings.

By designing a virtual prototype and manufacturing a physical prototype, the correctness and reliability of the robot parallel gripper design proposed in this study were verified. Overall, the experiments verified the effectiveness of the comprehensive approach proposed in this study for designing robot grippers.

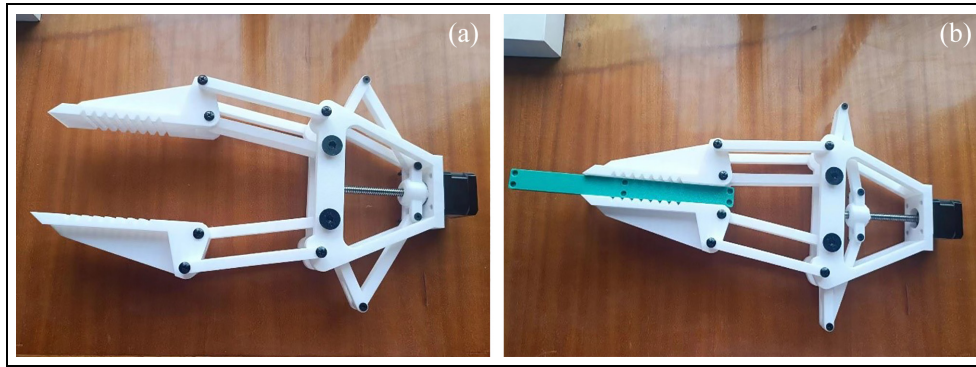


Figure 17. Robot gripper physical prototype: (a) physical prototype of the gripper and (b) the gripper holds an object.

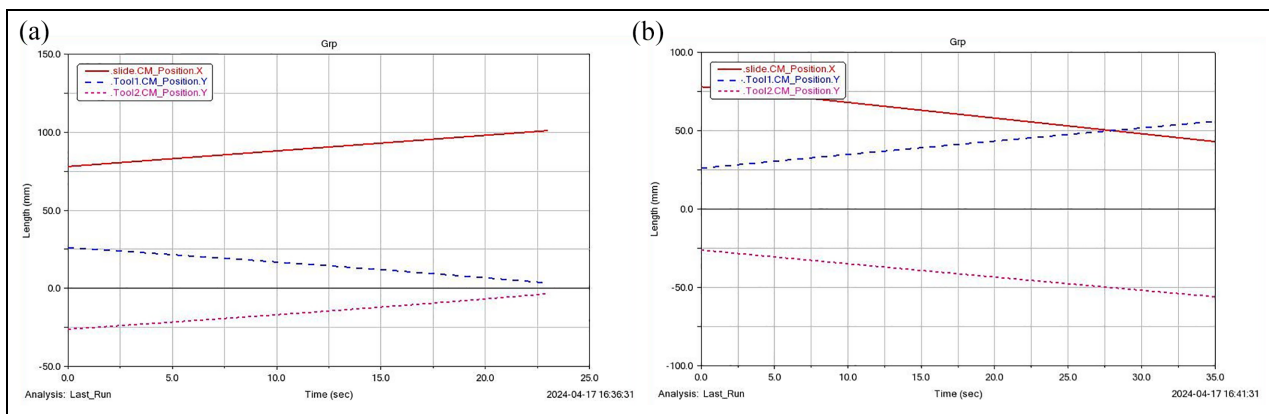


Figure 18. Displacement measurement of robot gripper: (a) motion curve of gripping task and (b) motion curve of separation process.

Conclusion

This study demonstrates the effectiveness of a comprehensive approach to robotic parallel gripper design optimization. By integrating improved BKA, FEA technology, and neural network model, gripper performance has been significantly improved. The improved group initialization and adaptive dynamic selection strategy in the improved BKA significantly improve the optimization efficiency. Through the population initialization of the GPS method, the BKA can explore a wider range of solutions from the beginning, preventing premature convergence to suboptimal solutions. Furthermore, the adaptive dynamic selection strategy ensures a balance between exploration and exploitation throughout the optimization process, enabling the algorithm to efficiently navigate complex solution environments and converge to high-quality solutions faster. These improvements make BKA more robust to changes in problem characteristics, thus enhancing its performance in different optimization tasks.

The utilization of FEA provides valuable insights into the structural integrity and performance of the

robotic gripper, allowing informed decisions to be made during the optimization process. The BKA-BPNN model was established to regression predict the performance of the parallelogram mechanism of the robot gripper under different design schemes. The RMSE of the neural network model training set and test set are 0.001615 and 0.0029328 respectively, which proves the effectiveness of the neural network model. The BKA-BPNN model provides numerical support for fitting the response surface design.

The application of response surface optimization helps determine optimal design parameters, thereby significantly improving fixture performance metrics. In this study, the maximum equivalent stress was reduced by 33.12%, the total mass was reduced by 1.47%, and the maximum total deformation was reduced by 0.16%. The developed fused neural network and response surface model provide a reliable framework to effectively explore the design space and guide the optimization process to achieve the desired performance goals.

The optimal design of the robot gripper needs to consider not only the gripping force, stability, and

structural strength, but also the material cost, manufacturing cost, assembly cost, and maintenance cost. This study did not involve research in this area. In the future, a cost model or cost function will be introduced as part of the optimization goal to achieve a balance between the performance and cost of the robot gripper by adjusting the design parameters, to achieve a more comprehensive and sustainable design and optimization of the robot gripper.

Overall, this study highlights the importance of a multidisciplinary approach to optimizing fixture design utilizing advances in improved BKA, FEA, BPNN, and response surface optimization techniques. The optimized robotic gripper design proposed in this study demonstrates the effectiveness of the proposed approach in enhancing gripper performance while reducing mass and improving structural integrity. Going forward, insights gained from this study can inform the development of more efficient and reliable robotic grippers for a wide range of industrial and research applications.

Acknowledgement

The authors would like to thank Universiti Putra Malaysia and Tianshui Normal University for their continuous support of the research work.

Declaration of conflicting interests

The author(s) declared no potential conflicts of interest with respect to the research, authorship, and/or publication of this article.

Funding

The author(s) disclosed receipt of the following financial support for the research, authorship, and/or publication of this article: Malaysian Fundamental Research Grant Scheme (FRGS) FRGS/1/2015/TK03/UPM/02/7 Fund (Grant No. 5524740), Tianshui Normal University Scientific Research Innovation Platform (No. PTJ2023-01) and Scientific Research Project (No. CXJ2022-05).

ORCID iDs

Ma Haohao  <https://orcid.org/0009-0001-6964-2357>
Mohd Idris Shah Ismail  <https://orcid.org/0000-0002-6254-0278>

Supplemental material

Supplemental material for this article is available online: <https://doi.org/10.6084/m9.figshare.27151227.v1>

References

- Söderlund M and Natorina A. Service robots in a multi-party setting: an examination of robots' ability to detect human-to-human conflict and its effects on robot evaluations. *Technol Soc* 2024; 77: 102560.
- Mani M, Murgaiyan T and Krishnan PK. Structural performance evaluation of hybrid polymer composites for critical infrastructure pick-and-place robot grippers using silica nanoparticles. *Int J Struct Integr* 2023; 14: 932–945.
- Ma H, Zhu S-P, Luo C, et al. Structural optimization design of metal rubber isolator based on an ensemble surrogate model. *Structures* 2023; 56: 104964.
- Vaisi B. A review of optimization models and applications in robotic manufacturing systems: Industry 4.0 and beyond. *Decis Anal J* 2022; 2: 100031.
- Jin T and Han X. Robotic arms in precision agriculture: a comprehensive review of the technologies, applications, challenges, and future prospects. *Comput Electron Agric* 2024; 221: 108938.
- Jung SH and Shin YS. Factors associated with intention to use care robots among people with physical disabilities. *Nurs Outlook* 2024; 72: 102145.
- Gao J, Zhang F, Zhang J, et al. Picking patterns evaluation for cherry tomato robotic harvesting end-effector design. *Biosyst Eng* 2024; 239: 1–12.
- Cvitanic T, Melkote S and Balakirsky S. Improved state estimation of a robot end-effector using laser tracker and inertial sensor fusion. *CIRP J Manuf Sci Technol* 2022; 38: 51–61.
- Chang Y-H, Liang C-H and Lan C-C. An end-effector wrist module for the kinematically redundant manipulation of arm-type robots. *Mech Mach Theory* 2021; 155: 104064.
- Dörterler M, Atila Ü, Top N, et al. A nested optimization approach for robot gripper multi-objective optimization problem. *Expert Syst Appl* 2024; 239: 122163.
- AboZaid YA, Aboelrayat MT, Fahim IS, et al. Soft robotic grippers: a review on technologies, materials, and applications. *Sens Actuators A Phys* 2024; 372: 115380.
- Wang J, Wang W-C, Hu X-X, et al. Black-winged kite algorithm: a nature-inspired meta-heuristic for solving benchmark functions and engineering problems. *Artif Intell Rev* 2024; 57: 98.
- Ouyang A, Li K, Fei X, et al. A novel hybrid multi-objective population migration algorithm. *Int J Pattern Recognit Artif Intell* 2015; 29: 1559001.
- Rasul A, Karuppanan S, Perumal V, et al. An artificial neural network model for determining stress concentration factors for fatigue design of tubular T-joint under compressive loads. *Int J Struct Integr* 2024; 15: 633–652.
- Yang S, Meng D, Wang H, et al. A novel learning function for adaptive surrogate-model-based reliability evaluation. *Philos Trans A Math Phys Eng Sci* 2024; 382: 20220395.
- Yang S, He Z, Chai J, et al. A novel hybrid adaptive framework for support vector machine-based reliability analysis: a comparative study. *Structures* 2023; 58: 105665.
- Wu Y-C and Feng J-W. Development and application of artificial neural network. *Wirel Pers Commun* 2018; 102: 1645–1656.
- Huang J, Nan J, Gao M, et al. Antenna modeling based on meta-heuristic intelligent algorithms and neural networks. *Appl Soft Comput* 2024; 159: 111623.

19. Zheng P, Zhang H, Zhang Z, et al. Parameter optimization method of contra-rotating vertical axis wind turbine: Based on numerical simulation and response surface. *J Clean Prod* 2024; 435: 140475.
20. Elsayed EW and Emam MF. Application of response surface methodology using face-centered central composite design for studying long-term stability of gliclazide-loaded multiparticulate systems. *J Pharm Sci* 2024; 113: 2274–2285.
21. Guezzen B, Medjahed B, Benhelima A, et al. Improved pollutant management by kinetic and Box-Behnken design analysis of HDTMA-modified bentonite's adsorption of indigo carmine dye. *J Ind Eng Chem* 2023; 125: 242–258.
22. Xue J and Shen B. Dung beetle optimizer: a new meta-heuristic algorithm for global optimization. *J Supercomput* 2023; 79: 7305–7336.
23. Heidari AA, Mirjalili S, Faris H, et al. Harris hawks optimization: algorithm and applications. *Future Gener Comput Syst* 2019; 97: 849–872.
24. Liu Y, As'array A, Hassan MK, et al. Review of the grey wolf optimization algorithm: variants and applications. *Neural Comput Appl* 2024; 36: 2713–2735.